A STUDY ON THE EFFECT OF LAMINATE TAPER ON DAMAGE MECHANISMS IN COMPOSITE LAMINATES

Lu Jin[1], Yong Chen[1,2], Jiguo Zhang[1], Xu Tang[1], and Jie Tian[1,2]

[1] School of Mechanical Engineering, Shanghai Jiao Tong University, Shanghai 200240, China
[2] Engineering Research Center of Gas Turbine and Civil Aero Engine, Ministry of Education, Shanghai 200240, China

Keywords: Composite laminate, Ply drops, Cohesive interface model, Delamination, Fatigue damage

ABSTRACT

Tapered laminates play a crucial role in achieving weight and aerodynamic efficiency in composite structures. However, their design can also introduce local material and geometric discontinuities, which can cause large interlayer stresses and become the site of damage initiation. Fatigue damage mechanisms of different taper angles laminates, designed by composite laminate design approach, were investigated by high-fidelity finite element modelling and a constitutive equation within the cyclic cohesive interface model approach. The different taper angles laminates were investigated at the first natural frequency under cyclic loading with different stress ratios to indicate the fatigue damage mechanisms. Weak-link index assessment was proposed to predict the location of fatigue damage, which was verified by the cyclic cohesive interface model approach. The results show that the maximum value of the damage index in dropped cohesive element plies is highly influenced by the taper angle. The taper angle is larger, and the stress is more concentrated, whereas a smaller taper angle results in a wider distribution of stress and stronger interaction between layers. The weak-link zone in these laminates is affected by the distribution of vibration stress, but sometimes nodes with low static stress can also become weak-link when subjected to static stress. Tapered laminates with a smaller taper angle are more prone to fatigue failure because the stronger interaction between layers and a wider range of stress distribution leads to a higher initial value of cumulative damage, which ultimately results in earlier fatigue failure.

1 INTRODUCTION

Fibre-reinforced plastic composites have become increasingly popular due to their exceptional mechanical properties, lightweight, design flexibility, and resistance to corrosion and fatigue [1]. To meet specific design requirements, composite components are often tapered along one or more directions. Tapered laminate allows for the creation of components with varying thickness and fibre orientation, providing the necessary strength and stiffness where required. This approach helps to optimize the weight and performance of the structure, resulting in greater efficiency and reduced operational costs [2].

A tapered composite laminate consists of layers known as "continuous plies" and "dropped plies", with the taper angle and several triangular resin pockets determined by the length and number of layers in the tapered region. Several studies have been conducted to develop guidelines and algorithms to optimize the design of such composites and reduce stress concentrations at the dropped plies. Mukherjee et al. [3] developed guidelines to guide the dropped plies design. Irisarri et al. [4] presented an evolutionary algorithm for dropped plies sequence optimization, which enabled satisfying design guidelines previously not considered. Sudhagar et al. [5] investigated the structural optimization of rotating tapered thick laminated composite plates using a genetic algorithm to obtain optimal ply sequence and orientation. However, there are few studies on the design of the composite fan blades dovetail for aero-engines or and only a few patents mention the design.

Despite their exceptional properties, composite laminates may sometimes fail to perform their intended functions due to various failure mechanisms such as fibre fracture, fibre pull-out, matrix cracking, and delamination. Delamination, in particular, is a prevalent form of failure that occurs both at the edges and in the interior of the laminate, especially under impact loads. As a result, numerous researchers have conducted extensive studies on composite laminates, utilizing both simulations and

experiments to investigate the failure mechanisms. The findings of these studies have important implications for the design and optimization of composite structures and can help to improve the safety and reliability of composite materials in a wide range of applications [6,7]. Various numerical methods have been developed over the years to predict the fatigue life of composite laminates, including fracture mechanics and continuum damage mechanics approaches [8,9]. However, these methods have traditionally faced challenges in integrating the damage initiation stage and crack propagation stage into a continuous process. To address this issue, researchers have proposed the use of cohesive zone models to simulate fatigue crack growth and demonstrate unloading-loading hysteresis. For instance, Maiti et al. [10] used a bi-linear CZM to simulate fatigue crack propagation in polymeric materials. The model was governed by an evolution law that related cohesive stiffness, rate of crack opening displacement, and loading cycles. One of the challenges with local versions of continuum damage mechanics models is that they often suffer from mesh pathological issues. As a solution to mitigate spurious mesh sensitivity in the modelling location, researchers have turned to nonlocal damage models [11,12]. Overall, the development of these numerical methods has enabled more accurate predictions of the fatigue life of composite laminates, helping to improve the design and performance of composite structures in various applications.

These studies have considered factors such as taper angle, the number of plies dropped, and fibre orientation. However, the issue of fatigue crack growth along the interfaces of tapered laminates has received less attention, especially under cyclic loading at the first natural frequency with different taper angles and weak-link zones. To address this gap in the literature, this study conducted an extensive numerical investigation and developed high-fidelity finite element models to better understand the failure mechanisms of tapered laminates under cyclic loading at the first natural frequency with different taper angles. The findings of this study could contribute to advancements in the field and help improve the design and performance of composite structures subjected to cyclic loading.

2 LAMINATE MODELLING

Composite laminates of different taper angles were designed to investigate the fatigue damage behaviour of composite fan blade dovetail in the preliminary study. A tapered laminates design approach was established based on the composite material layer design criterion and Fibresim® software, as shown in Fig. 1.

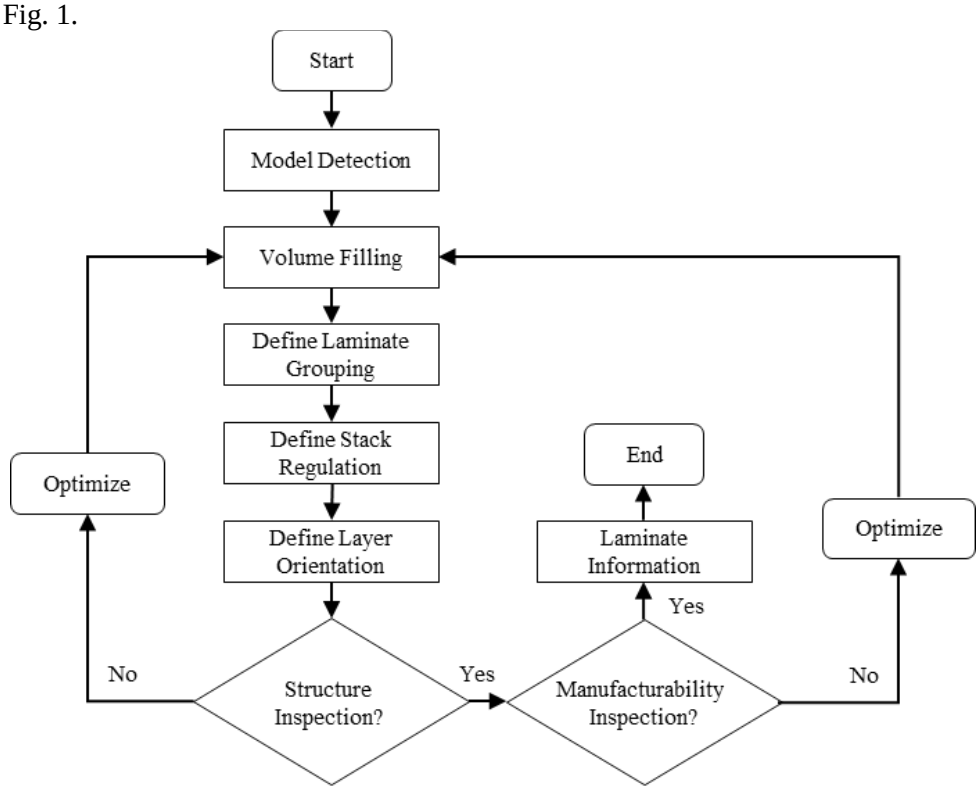

Figure 1: Flowchart of composite laminate design [13].

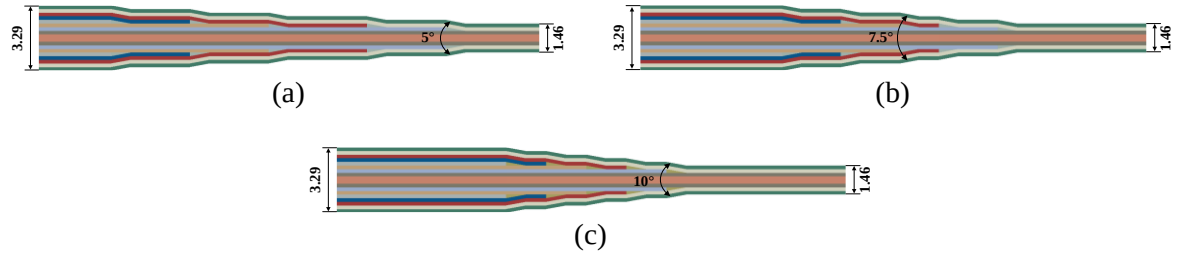

Figure 2: Schematics of (a) the 5° tapered laminate, (b) the 7.5° tapered laminate and (c) the 10° tapered laminate.

There are many styles in which a taper can be designed, it has already been described previously in detail. One area of significance is the design of the taper itself. The chosen ply style of tapered laminates is the shape of like “bamboo shoots shell” in this study, where the steps formed by the dropped plies are covered in a group of dropped plies by the layers within the group, so that all of the steps between a group of dropped plies and the adjacent plies are minimized, which will reduce the resin accumulation formed between the dropped plies and the adjacent plies during the curing process [13]. And based on that, the composite tapered laminates were mainly designed for three different taper angles in Fig. 2, where they have a total of 18 layers, including eight layers named “continuous plies” and ten layers named “dropped plies”.

Another area of significance is the design of the layup sequence. According to the layup sequence in Fig. 3(a), the resin deposition formed by dropped plies is all concentrated on both sides’ surfaces, which violates the design criterion for the transition area. Therefore, the ply sequence needs to be further optimized and adjusted. The number of layer orientations should be as small as possible to simplify the design and manufacture under the condition of satisfying the strength. Due to the main load of the fan blades in the aviation field being the centrifugal force along the blade height direction, the layer orientations of 0° and ±45° are used to maximize the high performance of the fibre axial direction.

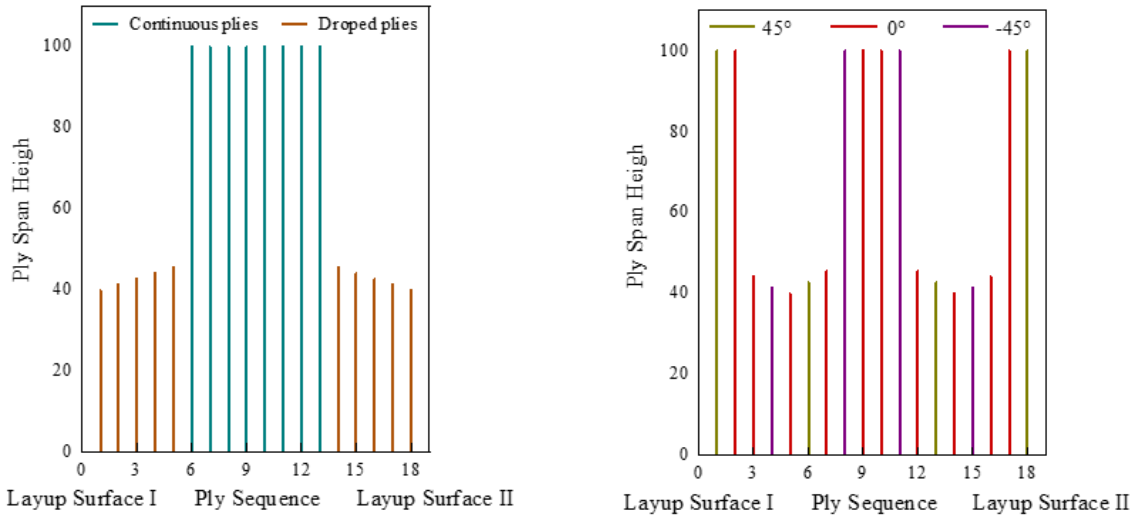

Figure 3: Comparisons between (a) original ply stacking sequence and (b) ply stacking sequence after shuffling.

Ply properties	E_{11} (MPa)	$E_{22}=E_{33}$ (MPa)	$G_{11}=G_{13}$ (MPa)	G_{23} (MPa)	$\nu_{11}=\nu_{13}$	ν_{23}
	161000	113800	5170	3980	0.32	0.32

Resin pocket properties	E (MPa)	ν	ρ (t/mm^3)
	3500	0.4	1.28e-09

Cohesive element properties	K_{I} (N/mm^3)	K_{II} (N/mm^3)	S_{I} (MPa)	S_{II} (MPa)	G_{I} (N/mm)	G_{II} (N/mm)	C_f	θ
	46700	17500	84	84	0.349	0.349	0.25	1.45

Table 1: The material properties of CYCOM®X850 Epoxy Resin System used in the tapered modelling.

According to the symmetry criterion, the layering order should be weighed on the middle face. The amount of work to select a reasonable layer order among many combinations is heavy, and appropriate simplification approaches are needed. The arrangement style of dropped plies orientation adopted is [0°/-45°/0°/45°/0°], with every five layers as a group of cyclic layers, and each group is laid in sequence according to the rule. Based on the above design criterion, which leads to a 1:2.25 thickness ratio between the thin and thick sections in Fig. 3(b). The results show that the laminate structure meets the requirements of the composite laminate design criterion, the progressive dropped plies and transition are rational, and the manufacturability is better.

The meshing tool used based on Composites Modeler for Abaqus® (CMA) software was further improved to create high-fidelity meshes after the tapered laminates design finish. Its mesh generation technique allows accurate representation of the entire tapered specimen, typically including post-cure ply thickness and slight ply waviness. All these tapered laminates models considered here follow some features has already been described previously in detail. The material properties used CYCOM® X850 in the models for prepreg layer and resin pockets are given in Table 1, which is ideal for use in primary aircraft structures where critical load-bearing components are required [14].

The tapered specimens did not show any matrix cracking or fiber breakage in the thickness direction before delamination occurred [2]. Therefore, this study focused solely on the delamination behaviour and used a cyclic cohesive interface model approach to develop a constitutive equation. This allowed for a more thorough examination of the failure criteria used to model the delamination failure, which was represented by a cyclic bi-linear traction-separation cohesive formulation. To analyze the interlaminar fatigue behaviour of the tapered laminate, the constitutive equations need to include damage initiation and evolution properties. The cyclic cohesive interface model approach is used to model the delamination failure of the laminate. The constitutive equations combine well-known characteristics of typical damage evolution laws [15]. The evolution equation for damage is written as follows, based on the above requirements.

$$\dot{D}_c = \frac{\left|\dot{u}_\Sigma\right|}{\delta_\Sigma}\left[\frac{T}{\sigma} - C_f\right]\psi\left(u_\Sigma - \delta_0\right),\ \dot{D}_c \geq 0 \tag{1}$$

Where represents the Heaviside function. The current damage evolution law is calculated by using effective cohesive quantities. The cyclic cohesive interface model as described in this study was implemented on Abaqus® software by the use of the USDFLD subroutine feature.

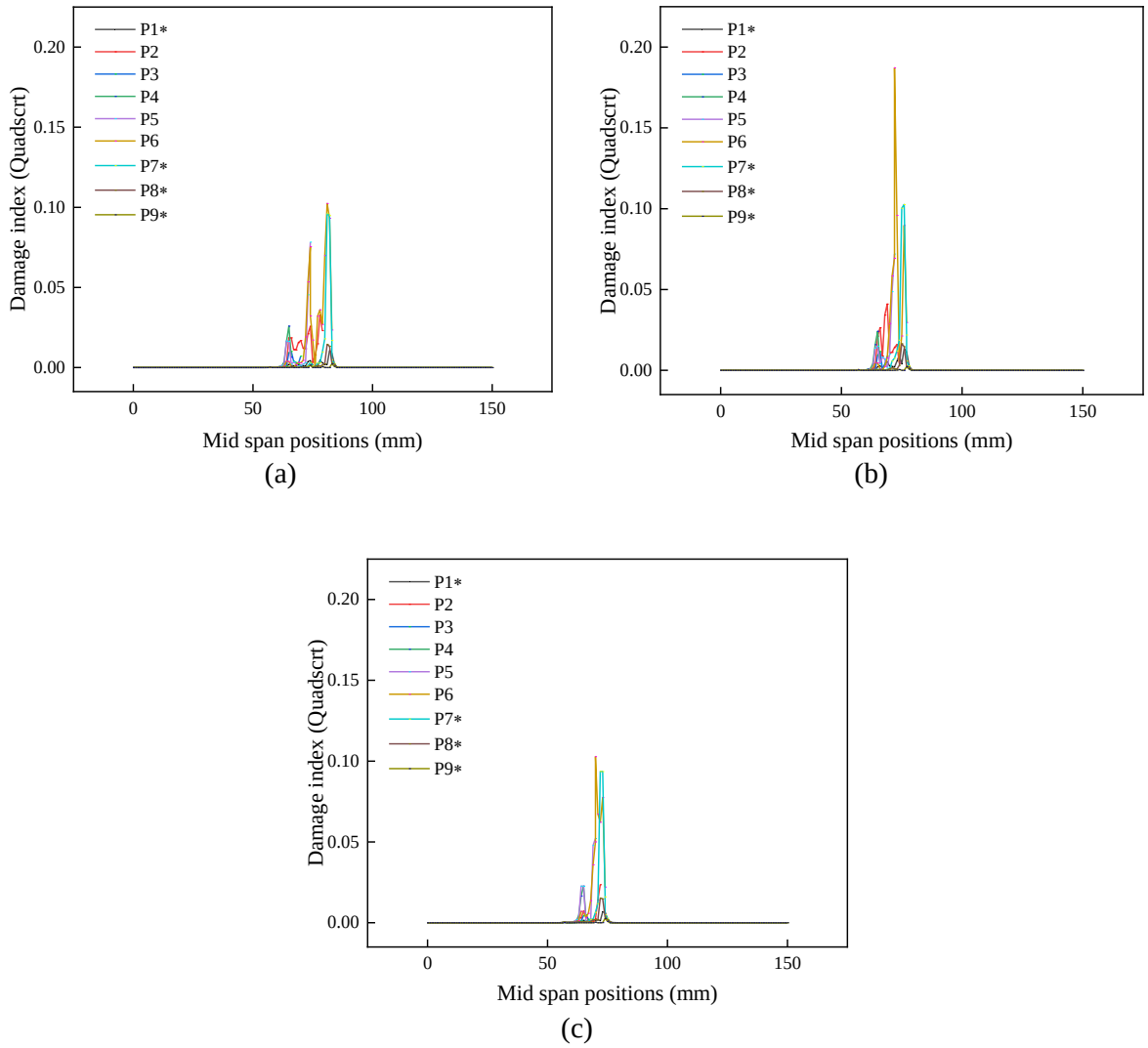

Figure 4: Comparisons of damage index between (a) 5° tapered laminate, (b) 7.5° tapered laminate and (c) 10° tapered laminate.

3 RESULTS AND DISCUSSION

3.1 Static damage assessment

Regarding monotonic loading, interlaminar behaviour is described by a bi-linear traction-separation cohesive formulation, which describes static damage initiation status in this section. Pure mode tractions (σ_n, σ_s and σ_t) and separations (δ_n, δ_s and δ_t) prior to failure are linearly related by an elastic stiffness (K_n, K_s and K_t). Damage initiation is applied based on the quads damage criterion when Eq. (2) is satisfied.

$$\left(\frac{\langle\sigma_n\rangle}{N_{\max}}\right)^2+\left(\frac{\langle\sigma_s\rangle}{S_{\max}}\right)^2+\left(\frac{\langle\sigma_t\rangle}{T_{\max}}\right)^2=1 \tag{2}$$

Where $N_{\max}$, $S_{\max}$ and $T_{\max}$ are the peak strength of mode I, mode II and mode III, respectively; the Macaulay operator $\langle\cdot\rangle$ defined as $\langle x\rangle=(1/2)(x+|x|)$.

When the load is applied by the numerical model with increased monotonic loading, the index of damage initiation increases from zero to one, resulting in interlaminar damage generation of tapered laminate eventually. When the load increases to 5kN, the damage index is used to assess the damage

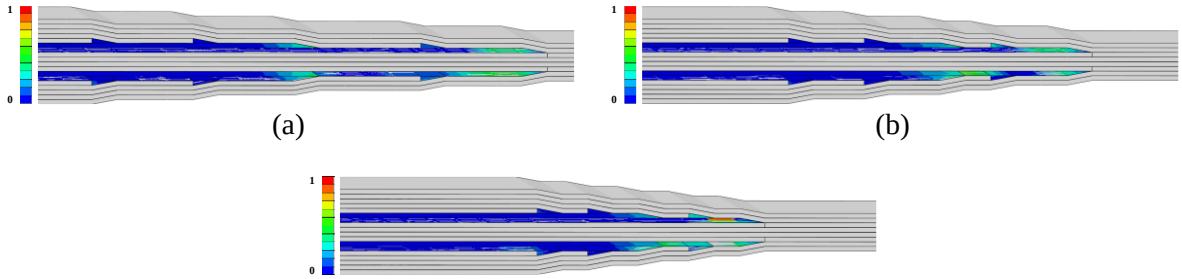

Figure 5: Comparisons of static damage index contour of (a) 5° tapered laminate, (b) 7.5° tapered laminate and (c) 10° tapered laminate.

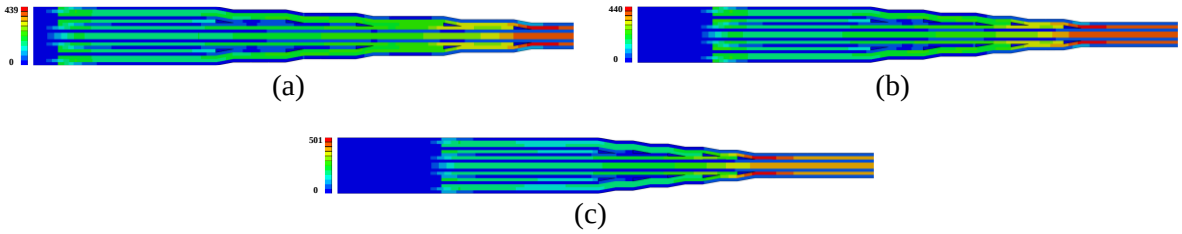

Figure 6: Comparisons of a stress contour plot of $S11$ direction under monotonic loading of (a) 5° tapered laminate, (b) 7.5° tapered laminate and (c) 10° tapered laminate.

initiation based on the quads damage criterion as shown in Fig. 4. Whatever type of three taper angles, all of the interface location of delamination initiated predicted is the same, which is located at the interface of dropped ply 7 and continuous ply 8 in continuous cohesive element plies, and interface of continuous ply 6 and dropped ply 7 in dropped cohesive element plies, as shown in Fig. 4. It can be seen that all of the maximum value of damage index in continuous cohesive element plies in three tapered laminate are approximately equal, but the maximum value of damage index in dropped cohesive element plies is different. Therefore, it indicates the maximum value of damage index in dropped cohesive element plies is more sensitive to taper angle change. It can also be seen that the range of stress distribution can increase with the decrease of the taper angle, which indicates the interaction of adjacent layers can be stronger. And another factor is that the stress can be more concentrated as the taper angle increase. These reasons ultimately lead to the highest damage index of 7.5° tapered laminate in dropped cohesive element plies in three tapered laminates.

The location of the maximum value of the damage index can be recognized as the ply interface of ply 6 to ply 7 in dropped cohesive element plies, and as the location of resin pocket in dropped cohesive element plies, as shown in Fig. 5. As the stress distribution in each layer is different under monotonic loading situations, which also indirectly leads to in different interlaminar stresses concentration in adjacent layers, as shown in Fig. 6.

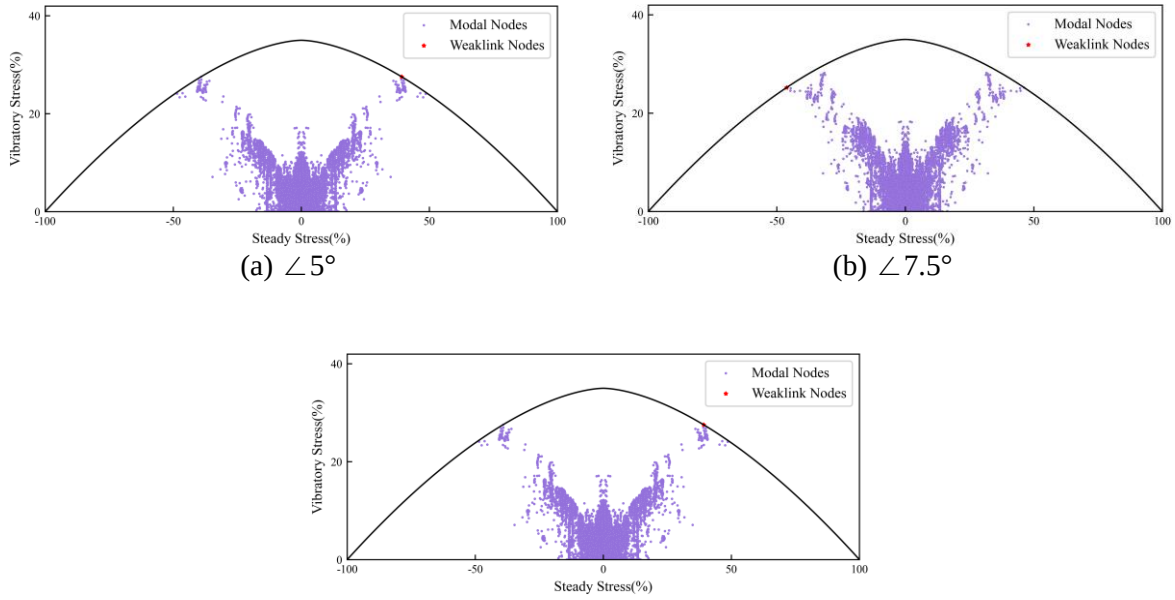

(a) ∠5° (b) ∠7.5°

(c) ∠10°

Figure 7: Comparisons of distribution of first-order flexure vibration stress margin on all nodes with $S13$ direction.

3.2 Dynamic damage assessment

This study developed a Goodman curve for composite laminates by incorporating the effects of tensile and compressive strength and average stress on fatigue life. The new model improves upon the classical constant life diagram model and allows for more accurate dynamic damage assessment. When designing for safety, it is important to consider not only the safety factor, but also the margin of vibration stress. By using the constant life diagram and Eq. (3), it is possible to locate and predict the weak-link in high-cycle fatigue.

$$\begin{cases} \sigma_{a,j} = \dfrac{\sigma_{f,j}}{\sigma_{c,j} - \sigma_{st,j}}\left(\sigma_{s,j} - \sigma_{st,j}\right), & \sigma_{c,j} \le \sigma_{s,j} \le \sigma_{st,j} \\ \sigma_{a,j} = \dfrac{\sigma_{f,j}}{\sigma_{c,j} + \sigma_{st,j}}\left(\sigma_{s,j} + \sigma_{sc,j}\right), & -\sigma_{sc,j} \le \sigma_{s,j} \le \sigma_{c,j} \end{cases} \tag{3}$$

The weak-link zone of each mode corresponds to the position, where the vibration stress margin reaches the minimum value, and this zone is the first to fail under a certain number of high-cycle fatigue cycles. Taking the calculation results of all directions of the first-order bending mode under the same load in three taper angles laminates, the weak-link zone is determined by both static and vibration stresses. For the calculation results of all directions of the first-order bending mode, the weak-link zone for all three taper angles laminates is located at the interface of ply 1 and ply 2, where the direction is located $S13$, which is determined mainly by vibration stresses, as shown in Fig. 7. In addition, the different steady stresses have a different weak-link zone, which is not discussed in details. In general, the distribution of vibration stress has a large impact on the weak-link zone, but the nodes with relatively small static stress values could be the weak-link zone, resulting from static stress applied to improve their vibration stress margin to a certain extent.

To investigate the first failure stress direction of tapered laminate under cyclic loading, the modal stress scaling factor value indicating damage index, which is normalized according to the relationship between the modal vibration stress in every direction and the allowable vibration stress ratio in the weak-link zone, as shown in Fig. 8. When the tapered laminate is in a certain vibration state, the stress direction with the largest scaling factor reaches its failure first. All of the maximum value of the scaling factor is the direction S13 of with different steady stress in three taper angles laminates. The scaling factor value

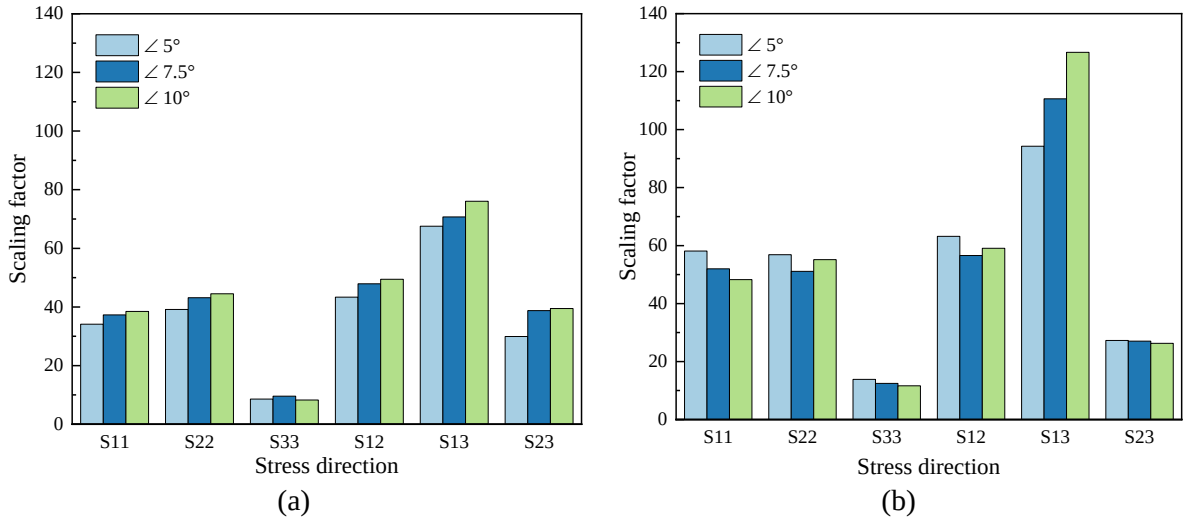

Figure 8: Comparisons of damage index of different static stress of (a) 1kN and (b) 5kN.

increases as the taper angles increase in the direction of $S13$ with different steady stress, which indicates interlaminar shear stress along the longitudinal orientations reaches its fatigue failure first, and also explains the reason why interlaminar failure is easier to break.

3.3 Fatigue behaviour

In this section, the interlaminar fatigue behaviour of the tapered laminate was investigated based on the constitutive equation with a cyclic cohesive interface model approach, where a schematic plot of loading is shown in Fig. 9.

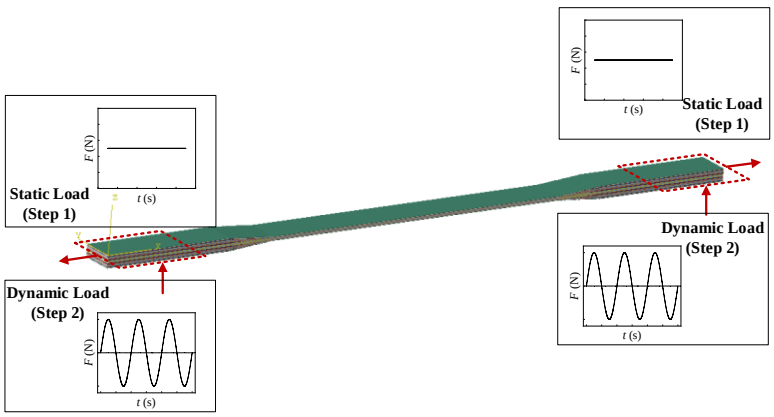

Figure 9: A schematic plot of the loading of fatigue behaviour of the tapered laminate [13].

There are two important parameters, which are time increment and coefficient of damage, as shown in Fig. 10. The effect of time increments with sampling frequencies ranging from $10T_f$ to $100f$ on crack area was investigated to reveal the damage mechanism better, as shown in Fig. 10(a). The less time increment is, the more damage accumulation is, which indicates fatigue crack growth rates is faster. Furthermore, the more coefficient of damage is, the more damage accumulation is, which indicates fatigue crack growth rates also is faster, as shown in Fig. 10(b). To accurately describe the dynamic load spectrum, the time increment needs to meet the sampling theory, and the coefficient of damage needs to be calibrated by experiment. Hence three times the first resonance frequency is used as the sampling frequency, and the sampling period is defined as the time increments.

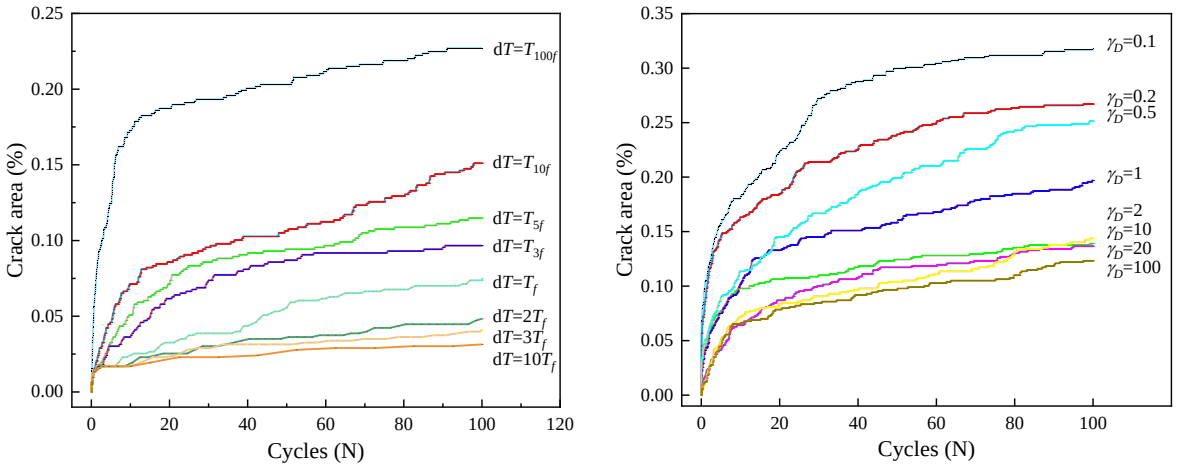

Figure 10: The effect of (a) time increment and (b) coefficient of damage on fatigue behaviour under amplitude of sinusoidal cyclic displacement.

To introduce the cyclic loading with different stress ratios, static stress is introduced as the mean stress and the amplitude of sinusoidal cyclic displacement is introduced as dynamic stress in this study. Fatigue crack growth is investigated at the first natural frequency under cyclic loading with different stress ratios with a target cycle number of 100 cycles. Taking the calculation results of the crack area in the taper angle of 7.5° laminate as an example, the fatigue behaviour is investigated for the amplitude of sinusoidal cyclic displacement ranging from 0.01mm to 1mm, which indicates the larger the amplitude of sinusoidal cyclic displacement under the same static stress, the faster the crack growth rate, as shown in Fig. 11(a). Furthermore, the larger the static stress under the same amplitude of sinusoidal cyclic displacement, the faster the crack growth rate. In addition, the effect of different taper angles on fatigue behaviour under the same amplitude of sinusoidal cyclic displacement is investigated, which has some unexpected results, as shown in Fig. 11(b). All of the calculation results with different taper angles share some features: (1) the crack growth rate only slightly increases as the taper angles increase, which indicates the range of the taper angles is not quite sensitive to the crack growth rate; (2) in the early stage of crack growth, the percentage of the crack area from large to small is 7.5°, 10°, 5°. One of the reasons is that the range of stress distribution can increase with the decrease of the taper angle, and the interaction of adjacent layers can be stronger, which results in the initial value of the cumulative damage being larger, and it fatigues failure first.

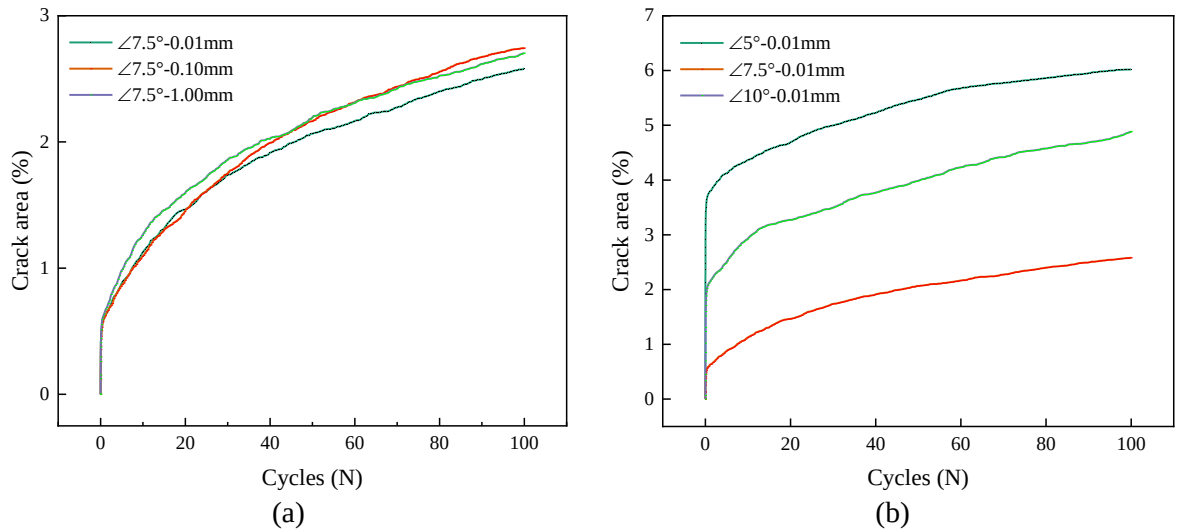

Figure 11: Comparisons of the behaviour of fatigue behaviour with the different dynamic loads.

4 CONCLUSIONS

This study focuses on the interlaminar fatigue behaviour of different taper angles laminates with a "bamboo shoots shell" shape under cyclic loading with varying stress ratios. The study proposes a novel tapered composite material layer design criterion, which shows that the laminate structure meets the composite laminate design criterion, has rational dropped plies and transition and is more manufacturable. The study also presents a static damage assessment method based on a bi-linear traction-separation cohesive formulation, which identifies the maximum damage index at the ply interface in dropped cohesive element plies. Additionally, a dynamic damage assessment method based on the classical constant life diagram model is proposed to predict the high-cycle fatigue weak-link zone. The results found that the maximum value of the damage index in dropped cohesive element plies is highly influenced by the taper angle. A smaller taper angle leads to a wider range of stress distribution and stronger interaction between adjacent layers, while a larger taper angle results in more concentrated stress. The weak-link zone in composite laminates is strongly affected by the distribution of vibration stress. However, nodes with relatively low static stress values can become weak-link zone due to the application of static stress, which can help to improve their vibration stress margin to some extent. Furthermore, the reason why tapered laminates with a smaller taper angle are more prone to fatigue failure is due to the stronger interaction between adjacent layers and the larger range of stress distribution. This leads to a higher initial value of cumulative damage and ultimately results in earlier fatigue failure. While this study successfully used a cyclic cohesive interface model approach to investigate fatigue delamination damage in composite laminates, there are limitations to this approach when it comes to high-frequency vibration and high stress or strain gradients. In particular, the approach may not accurately simulate fatigue delamination growth in the dropped plies area of tapered laminates. To address this limitation, future research may need to propose a bond damage model within peridynamics that can better capture nucleation and growth of cracks in composite tapered laminates. Additionally, experimental validation will be necessary to fully quantify and understand the fatigue failure mechanisms of these materials.

ACKNOWLEDGEMENTS

The authors would like to acknowledge the Engineering Research Center of Gas Turbine and Civil Aero Engine for the support of this research through the School of Mechanical Engineering at Shanghai Jiao Tong University, China.

REFERENCES

[1] He K, Hoa SV, Ganesan R. The study of tapered laminated composite structures: a review. *Compos Sci Technol* 2000; 60: 2643-57.

[2] Bing Z, Luiz F, Mike A. An experimental and numerical investigation into damage mechanisms in tapered laminates under tensile loading. *Composites Part A: Applied Science and Manufacturing* 2020; 133.

[3] Mukherjee A, Varughese B. Design guidelines for ply drop-off in laminated composite structures. *Composites Part B Engineering* 2001; 32(2): 153-164.

[4] Irisarri F X, Lasseigne A, Leroy F H. Optimal design of laminated composite structures with ply drops using stacking sequence tables. *Composite Structures* 2014; 107: 559-569.

[5] Sudhagar P E, Babu A A, Rajamohan V. Structural optimization of rotating tapered laminated thick composite plates with ply drop-offs. *International Journal of Mechanics and Materials in Design* 2017; 13(1): 85-124.

[6] Carraro P A, Novello E, Quaresimin M, et al. Delamination Onset in Symmetric Cross-Ply Laminates Under Static Loads: Theory, Numerics and Experiments. *Composite Structures* 2017; 176: 420–432.

[7] Bak B L, Turon A, Lindgaard E, et al., A Simulation Method for High-Cycle Fatigue-Driven Delamination Using a Cohesive Zone Model. *International Journal for Numerical Methods in Engineering* 2016; 106(3): 163-191.

[8] Brod M, Dean A, Rolfes R. Numerical life prediction of unidirectional fiber composites under block loading conditions using a progressive fatigue damage model. *International Journal of Fatigue*, 2021, 147: 106159.

[9] Gerendt C, Dean A, Mahrholz T, et al. On the progressive fatigue failure of mechanical composite joints: Numerical simulation and experimental validation. *Composite Structures*, 2020, 248: 112488.

[10] Maiti, S., Geubelle, P.H. A Cohesive Model for Fatigue of Polymers. *Engineering Fracture Mechanics* 2005; 69(5): 691-708.

[11] Kumar P K A V, Dean A, Reinoso J, et al. A multi phase-field-cohesive zone model for laminated composites: Application to delamination migration. *Composite Structures*, 2021, 276: 114471.

[12] Kumar P K A V, Dean A, Reinoso J, et al. Phase field modeling of fracture in Functionally Graded Materials: Γ-convergence and mechanical insight on the effect of grading. *Thin-Walled Structures*, 2021, 159: 107234.

[13] Jin L, Chen Y, Tang X, et al. A numerical study on damage characteristics in composite tapered laminates under cyclic loading with different stress ratios. *Composite Structures*, 2023, 311: 116777.

[14] Zhang B, Allegri G, Yasaee M, Hallett SR, Partridge IK. On the strain and delamination sensing functions of CFRP Z-pins. *Compos Sci Technol* 2015; Under Revi:1-25.

[15] Lemaitre J. A Course on Damage Mechanics. *Berlin: Springer-Verlag* 1996.